X-Ray Diffraction and X-Ray Spectroscopy Studies of Cobalt-Doped Anatase TiO2:Co Nanopowders

Mesilov, V. V.; Galakhov, V. R.; Gubkin, A. F.; Sherstobitova, E. A.; Zakharova, G. S.; Uimin, M. A.; Yermakov, A. E.; Kvashnina, K. O.; Smirnov, D. A.;

Originally published:

October 2017

Journal of Physical Chemistry C 121(2017)43, 24235-24244

DOI: https://doi.org/10.1021/acs.jpcc.7b05873

X-Ray Diffraction and X-Ray Spectroscopy Studies of Cobalt-Doped Anatase TiO_2:Co Nanopowders

V. V. Mesilov,[†] V. R. Galakhov,[*,†] A. F. Gubkin,[†,‡] E. A. Sherstobitova,[†,¶] G. S. Zakharova,[§] M. A. Uimin,[†,‡] A. E. Yermakov,[†,‡] K. O. Kvashnina,[‖,⊥] and D. A. Smirnov[#]

M. N. Miheev Institute of Metal Physics, Ural Branch of the Russian Academy of Sciences, 620137 Yekaterinburg, Russia, Institute of Natural Sciences, Ural Federal University, 620083, Yekaterinburg, Russia, Institute of High-Temperature Electrochemistry, Ural Branch of the Russian Academy of Sciences, 620137 Yekaterinburg, Russia, Institute of Solid State Chemistry, Ural Branch of the Russian Academy of Sciences, 620137 Yekaterinburg, Russia, Rossendorf Beamline at ESRF — The European Synchrotron, CS40220, 38043 Grenoble Cedex 9, France, Helmholtz Zentrum Dresden–Rossendorf (HZDR), Institute of Resource Ecology, PO Box 510119, 01314 Dresden, Germany, and Helmholtz-Zentrum Berlin für Materialien und Energie, BESSY II, 12489 Berlin, Germany

E-mail: galakhov@ifmlrs.uran.ru

[*]To whom correspondence should be addressed
[†]Institute of Metal Physics
[‡]Ural Federal Univsersity
[¶]Institute of High-Temperature Electrochemistry
[§]Institute of Solid State Chemistry
[‖]European Synchrotron Radiation Facility
[⊥]Helmholtz Zentrum Dresden–Rossendorf
[#]Helmholtz-Zentrum Berlin für Materialien und Energie

Abstract

Cobalt-doped anatase $Ti_{0.97}Co_{0.03}O_2$ nanopowders with a particle size of about 100 Å were produced by a microwave-hydrothermal method. The obtained samples were characterized by means of X-ray diffraction, X-ray absorption (Ti $L_{2,3}$, Co $L_{2,3}$, and Co K), and 1s3p resonant inelastic X-ray scattering spectroscopies. Co^{2+} ions tetrahedrally coordinated by oxygen ions in nanoparticles were found to be located on the surface of agglomerates. Titanium ions were found to be in a tetravalent state (Ti^{4+}). All the samples before the thermal treatment contain an amorphous phase of titanium dioxide on the surface. After annealing in vacuum or hydrogen anatase structure of $Ti_{0.97}Co_{0.03}O_2$ remains and the amorphous phase disappears. Annealing the samples in vacuum or hydrogen leads to clustering metal cobalt at the particles from the bulk of agglomerates.

Introduction

Co-doped TiO_2 is one of the most extensively studied oxides for applying as dilute magnetic semiconductors.[1,2] One of the important tasks for creating spintronic devices is to learn to achieve a high transition temperature in the ferromagnetic state in magnetic semiconductors so that the devices can work at room temperature. For the first time ferromagnetism at room temperature in Co: TiO_2 with an anatase structure was recorded in.[3]

There are at least two points of view on the origin of ferromagnetism in this material: (i) ferromagnetism in TiO_2:Co originates from the presence of Co clusters,[4] (ii) ferromagnetism is intrinsic nature.[5] Therefore, oxidation state of cobalt is of particular interest in such materials. The majority of works on elucidating the nature of appearance of spontaneous magnetization with a high Curie temperature in doped TiO_2 oxides and other magnetic semiconductors was performed on bulk states. It can be assumed that in the nanocrystalline TiO_2:Co oxide powders, the above physical phenomena will manifest themselves particularly vividly in comparison with massive objects due to the specific contribution of the surface

and the specificity of the electronic structure of the cobalt impurities.

It should be noted that the fundamental feature of the nanostate is the thermodynamically justified localization of 3d impurities and defects over anionic and cation sublattices on the surface of nanoparticles. The dominant contribution of the surface in the nanocrystalline nonequilibrium state will be decisive in the formation of physicochemical properties of titanium dioxide with cobalt impurities. The elucidation of this problem requires the determination of the charge and spin states, as well as the crystal environment of cobalt ions in the TiO_2 anatase lattice.

Effective methods for studying the surface states of ions in 3d metal oxides is soft X-ray absorption spectroscopy in total electron yield mode. Whereas bulk states studies can be studied using hard X-ray absorption and emission spectra. The extension of the core-hole lifetime present in the XAS measurements can be significantly reduced by measuring X-ray absorption in the high-energy fluorescence detection mode (HERFD). The lifetime of the observed state is increased by choosing only one transition associated with the lifetime, which is necessarily longer than the lifetime of the excited state. Combination of absorption and emission is often viewed as resonant inelastic X-ray scattering (RIXS).[6] In the RIXS process, the internal electron is excited to an unoccupied valence level. The system is excited and de-excited for usually several femtoseconds. We note that the charge of the system does not change in the process, i. e., an electron is not lost or added. The process can be viewed as an inelastic scattering of the incident photon at the 3d transition metal atom and is theoretically described by the Kramers-Heisenberg formula.[7] RIXS depends on the energy of incoming and outgoing photons, so the full RIXS image is two-dimensional.

Hard X-ray spectral studies of titanium dioxide with cobalt impurities are presented in a series of papers.[8–11] According to experimental and theoretical Co K X-ray absorption spectra, that cobalt ions in thin TiO_2 films are found to be located mainly in interstices in the anatase lattice and form complexes with titanium ions and vacancies in oxygen.[8] Yildirim et al.[9] have studied an amorphous and polycrystalline states of TiO_2:Co, as well as

in the form of thin films. In the amorphous phase of TiO_2:Co, cobalt ions are in a divalent state with mixed coordination of atoms, and in polycrystalline and thin films, Co^{2+} ions are in an octahedral environment with tetragonal distortion and replace in this case titanium ions in the anatase lattice of TiO_2:Co.[9] According to Co K X-ray absorption spectra, cobalt atoms in thin films of rutile TiO_2:Co with a rutile structure are located at titanium positions with the formation of vacancies as a result of annealing.[10] Substitution of Ti^{4+} ions for Co^{2+} leads to the formation of vacancies in oxygen sublattice.[11]

Soft X-ray spectral studies of Co-doped titanium dioxide were presented in the works.[11–17] It was shown by means of X-ray photoemission spectra that cobalt in thin films $Co_xTi_{1-x}O_2$ is in a divalent state.[12] It was found that annealing in oxygen of thin anatase TiO_2 films doped with cobalt led to the formation of metallic cobalt and its clustering.[13] The authors of[11] have investigated Ti L X-ray absorption spectra of $Ti_{1-x}Co_xO_{2-\delta}$ and concluded that doping with cobalt ions leads to a distortion of the TiO_2 structure. It was shown from Co L X-ray absorption spectrathat in thin TiO_2 films with 3d impurities, cobalt in the depth of the film is in the metallic state and on the surface in the oxidized state[14] . Using X-ray photoelectron spectroscopy, it was the authors of established the presence of metallic cobalt in $Co_{0.2}Ti_{0.9}O_2$ after annealing in hydrogen,[15] unlike $Co_{0.1}Ti_{0.9}O_2$ subjected to heating under the same conditions. Mamiya et al.[16] have established from comparison of X-ray dichroism spectra of and atomic multiplet calculation that in thin films, $Ti_{1-x}Co_xO_{2-\delta}Co^{2+}$ ions are located at titanium positions in the high-spin state in a crystal field with the symmetry D_{2h}. According to X-ray photoelectron and absorption Co L spectra measured by Parma et al.,[17] cobalt is in a divalent state, mainly in phases, which after annealing form islands in the near-surface layer of thin TiO_2 films doped with cobalt.

The spectra of resonant inelastic X-ray scattering of TiO_2:Co nanopowders are not presented in the literature and will be investigated in this paper for the first time. Soft X-ray absorption spectra will be given in comparison with calculations of atomic multiplets taking into account the crystal field. On the one hand, soft X-ray spectra will provide information

on nanoparticles in the nanoscale agglomerates in the near-surface layer (5-10 nm). On the other hand, hard X-ray spectra will allow to determine the degree of oxidation of cobalt ions in particles in the volume of agglomerates.

Experiment and Details of Muliplet Calculations

Nanopowders of titanium dioxide with cobalt impurities were obtained by a microwave-hydrothermal method. As the starting materials, a 15% solution of titanium (III) chloride in a 10% solution of HCl from Merck, cobalt (II) chloride $CoCl_2 \cdot 6H_2O$ and a 25% water solution of ammonia were taken. The samples of TiO_2 with cobalt impurities were synthesized as follows: the calculated amount of $CoCl_2 \cdot 6H_2O$ was dissolved in water, then a stoichiometric amount of $TiCl_3$ was added to the solution. To the resulting reaction mixture, NH_4OH was added dropwise until $pH = 9.2$. The process was carried out with constant stirring. Then the reaction mass was subjected to ultrasonic treatment using ultrasonic bath UZV-1.3 TTS "Sapphire" for 20 min. The resulting slurry was placed in a Monowave 300 reactor (Anton Parr), heated to 160 °C and held at this temperature for 20 minutes. The resulting precipitate was filtered off, washed with water and air dried at room temperature. The obtained samples were annealed in vacuum and hydrogen for 2 hours at a temperature of 700 °C. To analyze the chemical composition of the powders, the inductively coupled plasma method was used. The concentration of cobalt in the samples was estimated to be about 3 at. % relative to the cation content. Therefore, the chemical formula of the obtained samples should be written as $Ti_{0.97}Co_{0.03}O_2$.

The crystal structure and the phase purity of the as-synthesized and annealed samples were checked by a powder X-ray diffraction using a Rigaku Dmax-2200 diffractometer with Cu Kα radiation ($\lambda = 1.54178$ Å). The Bragg lines broadening due to the microstructural effects was analyzed by means of the Rietveld refinement using TCH pseudo-Voigt peak profile function.[18] The Reitveld refinement was performed using Fullproff software package.[19]

The instrumental resolution function was obtained to be $u = 0.00708$, $v = -0.00832$, $w = 0.03468$ in terms of Cagliotti formula[20] by fitting of the X-ray diffraction pattern measured on the Al_2O_3 standard sample. Visualization of the coherently scattering domain has been performed using GFOURIER program.[21]

Ti $L_{2,3}$ and Co $L_{2,3}$ X-ray absorption (XAS) spectra of were obtained at Russian-German beamline at BESSY (Berlin) in the surface-sensitivity total photoelectron-yield mode. All the spectra were normalized to the beam flux measured by a clean gold mesh.

Co K X-ray absorption spectra were collected in high energy resolved fluorescence detection (HERFD) mode at room temperature, using the Rossendorf Beamline (ROBL, BM-20) at the European Synchrotron Radiation Facility (ESRF). The samples, the analyzer crystal and the photon detector (avalanche photodiode) were arranged in the vertical Rowland geometry. The core-to-valence RIXS spectra were recorded at a scattering angle of 90 °C in the horizontal plane using only one crystal analyzer. The intensity was normalised to the incident flux. Experiment was performed at room temperature in helium atmosphere. The extension of the life-time in the core-hole, which is present in XAS measurements, can be significantly reduced by measuring XAS in high-resolution fluorescence (HERFD) mode.[22] Increased the lifetime of the observed state by choosing only one transition associated with the lifetime, which, by virtue of the need is greater than the full service life of the excited state.

Crystal-field multiplet calculations of $L_{2,3}$ XAS spectra for Co ions in oxygen octahedral (O_h) and tetrahedral (T_d) environments were carried out using a computer program for calculation of spectra with a multiplet structure determined by the Coulomb and exchange interactions between 2p holes and 3d electrons, the splitting by the crystal field, and spin–orbit interaction.[23,24] The calculation of theoretical Co L spectra was carried out in two stages. At the first stage, the spectrum of a purely atomic multiple was calculated. As a parameter, only the atomic number was included and the transition $2p^63d^n \rightarrow 2p^53d^{n+1}$ was taken into account. The absolute value of the transition energy was not calculated. The

energies of the calculated spectra were brought into correspondence with the energies of the experimental spectra. In the second stage, the Slater–Condon parameters for the direct Coulomb interaction and the exchange Coulomb interaction were included through the Slater integrals F_{dd}, F_{pd}, and G_{pd}, which were calculated by the Hartree–Fock method. The value of the Slater integrals was taken equal to 80% of the atomic values for cobalt ions. Slater integrals were calculated by the Hartree–Fock method. Crystal field parameters ($10Dq$) were taken identical for the basic and final states of the system. The crystal field parameter 10Dq (the splitting value between the e_g and t_{2g} orbitals) was taken equal to 0.8 eV for the octahedral environment. For the tetrahedral environment, orbitals e_g are situated at lower energy than the t_{2g} ones, therefore the parameter 10Dq has a negative sign and was equal to -0.6 eV. Taking into account that $L_{2,3}$ X-ray absorption spectra are dominated by multiplet,[25,26] we neglect charge-transfer effects in our calculations of $L_{2,3}$ X-ray absorption spectra.

Results

X-ray diffraction analysis

X-ray diffraction data measured on the as-prepared pure TiO_2 nanopowder and as-synthesized, annealed in vacuum and annealed in hydrogen Co-doped $Ti_{0.97}Co_{0.03}O_2$ nanopowder samples are shown in Fig. 1(a)–(d). The X-ray diffraction patterns of both the as-synthesized samples can be well indexed by the crystal structure model of anatase (space group I41/amd).[27] A trace amount of the impurity phase, which was identified as brookite (PDF #29-1360), was observed on the X-ray diffraction pattern for pure TiO_2. We did not observe any extra reflections on the X-ray diffraction pattern for the as-synthesized $Ti_{0.97}Co_{0.03}O_2$ sample. Contrary, the $Ti_{0.97}Co_{0.03}O_2$ samples annealed in vacuum and in hydrogen atmosphere revealed additional Bragg peaks which can be indexed by the TiO_2 rutile phase (PDF #84-1285) and fcc metallic Co phase (PDF #89-7093). Broad background humps as well as reduced peak-to-

background ratio observed for the as-synthesized $Ti_{0.97}Co_{0.03}O_2$ sample implies substantial scattering contribution from amorphous phase.

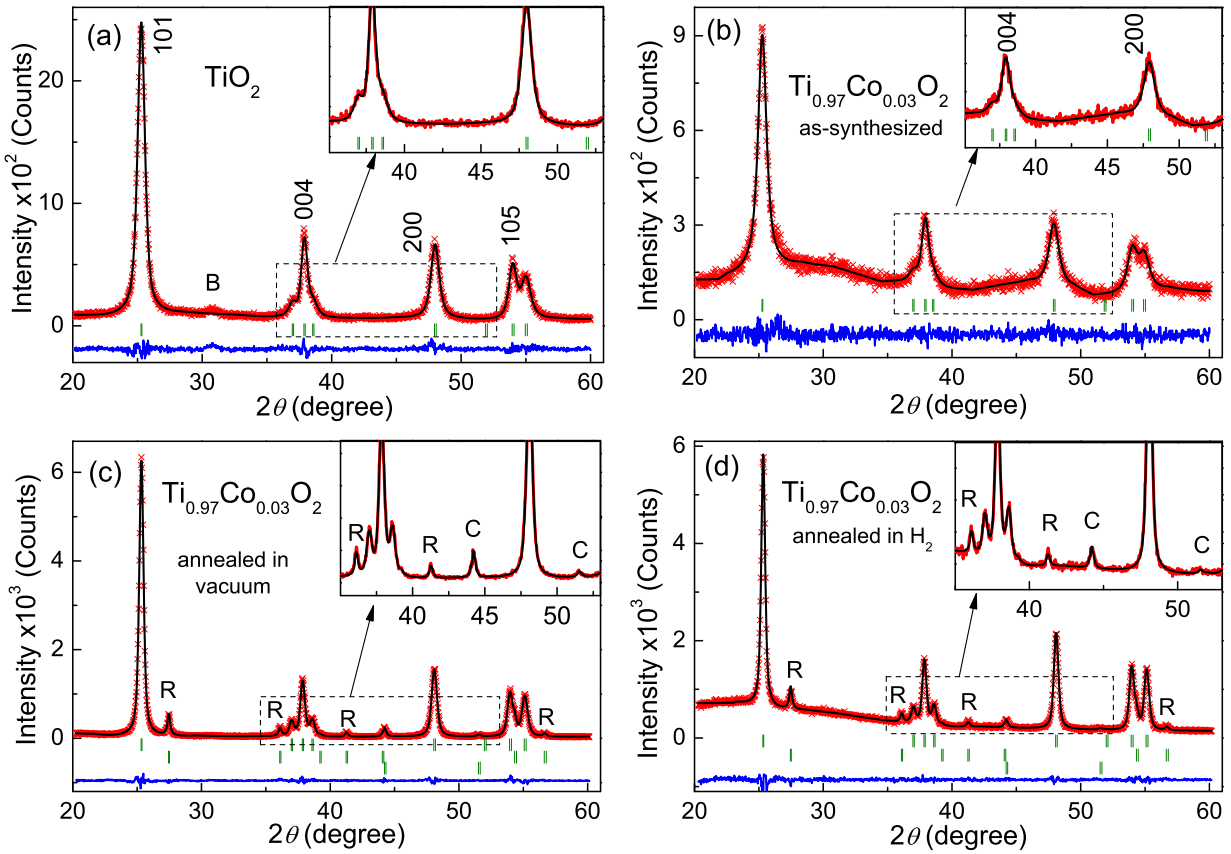

Figure 1: The best fit result for the X-ray diffraction patterns measured for (a) as-synthesized TiO_2 sample, (b) as-synthesized $Ti_{0.97}Co_{0.03}O_2$ sample, (c) $Ti_{0.97}Co_{0.03}O_2$ sample annealed in vacuum, (d) $Ti_{0.97}Co_{0.03}O_2$ sample annealed in hydrogen. Red symbols are experimental values of the intensity and black solid line represents the result of the fit. The difference curve between calculated and observed intensities is shown at the bottom. The rows of vertical marks below the patterns refer to the Bragg angles of the anatase structure (upper row), rutile structure (middle row), fcc Co phase (bottom row). Symbols "R", "C" and "B" mark rutile, cobalt and brookite peaks, respectively (see the text).

Strong broadening of the Bragg lines of the anatase structure in comparison with the instrumental resolution function was observed for all the measured X-ray diffraction patterns. Such broadening implies that both size as well as microstrain effects may be crucial for these samples. In order to estimate size and strain effects contribution and clarify how microstructural effects in the $Ti_{0.97}Co_{0.03}O_2$ nanoparticle sample evolves on annealing, we

performed microstructural analysis by means of the Rietveld refinement using Fullprof software package.[19] The integral breadth approach to obtain apparent size and microstrain for each Bragg peak is employed in Fullprof.[28,29] The average maximum strain calculated in Fullprof corresponds to 1/4 of the apparent strain in terms of Stokes and Wilson.[30] Size and microstrain effect contributions to the integral breadth of Bragg peaks are calculated on the Rietveld refinement using TCH pseudo-Voigt peak profile function (see Fullprof manual for details).

The crystal structure of anatase (space group $I41/amd$)[27] along with isotropic size and strain contributions were taken as a trial model for the Rietveld refinement of the as-synthesized samples. Occupation factors for Ti and Co statistically distributed over 4b Wyckoff site of anatase structure were fixed to the numbers obtained from the chemical analysis. It has been found that broadening of Bragg lines for the as-synthesized sample exhibits anisotropic character and cannot be well approximated by the isotropic microstructural effects. In particular, the integral breadth for the (004) Bragg peak is substantially narrower than the one for the peaks (101) and (200) (see Table 1). In order to describe anisotropic broadening of Bragg lines, anisotropic size effect was modeled using spherical harmonics approximation implemented in Fullprof:[28,29]

$$\beta^{sz}_{hkl} = \frac{\lambda}{D_{hkl}\cos\theta} = \frac{\lambda}{\cos\theta}\sum_{lmp} a_{lmp} y_{lmp}(\Theta_{hkl}, \Phi_{hkl}), \tag{1}$$

where $\sum_{lmp} a_{lmp} y_{lmp}(\Theta_{hkl}, \Phi_{hkl})$ is a linear combination of spherical harmonics as it was described in Ref.[31] After refinement of the coefficients a_{lmp}, apparent size of the coherently scattering domain along the direction that is perpendicular to the scattering plane (hkl) can be calculated. Then average apparent size over N measured Bragg peaks $\langle D_{hkl}\rangle = \frac{1}{N}\sum_{hkl} D_{hkl}$ and its standard deviation $\sigma\langle D_{hkl}\rangle$, that is a measure of the degree of anisotropy of the diffraction domain, are calculated by Fullprof. The parameters obtained on the refinement of the anatase structure model with isotropic microstrain and anisotropic size contributions are represented in Table 1. The difference between observed and calculated profiles for

Table 1: The refined unit cell parameters of anatase structure a and c, $\langle D_{hkl}\rangle$ — average apparent size of the difraction domain and its standard deviation $\sigma\langle D_{hkl}\rangle$, e — average maximum strain, β_{hkl} — integral breadth of the Bragg peak (hkl) in terms of TCH-pV profile function, χ^2 — square of goodness of fit, $R_{\rm RWP}$, $R_{\rm REXP}$ — agreement factors corrected for background.

	TiO_2	$Ti_{0.97}Co_{0.03}O_2$		
	as-synth	as-synth	annld. vacuum	annld. hydrogen
$a(\Delta a)$ [Å]	3.7912(3)	3.7970(7)	3.7844(1)	3.7839(1)
$c(\Delta c)$ [Å]	9.4972(6)	9.4901(16)	9.5055(3)	9.5063(3)
$\langle D_{hkl}\rangle$ $(\sigma\langle D_{hkl}\rangle)$ [Å]	103 (18)	92.4 (15)	197 (10)	244 (0)
e[%]	0.097	0.382	0.152	0.138
$\beta_{(101)} \times 10^3$ [Å^{-1}]	9.92	12.68	5.07	4.29
$\beta_{(004)} \times 10^3$ [Å^{-1}]	6.99	9.29	5.29	4.50
$\beta_{(200)} \times 10^3$ [Å^{-1}]	10.92	13.42	6.00	4.70
$\beta_{(105)} \times 10^3$ [Å^{-1}]	9.18	12.10	5.75	4.83
χ^2	1.5	1.2	1.3	1.2
$R_{\rm WP}$	12.3	22.0	8.7	9.6
$R_{\rm EXP}$	10.2	20.2	7.7	8.9

each sample is shown in Figures 1(a)–(d). Visualizations of the average apparent diffraction domain drawn by GFOURIER program are shown in Figures 2(a)–(d) for all the studied samples. It should be emphasized that little physical meaning comes from the particular shape of the diffraction domain. A particular shape is an extrinsic property defined by the sample synthesis method rather than an intrinsic property of the material.

Ti $L_{2,3}$ X-ray absorption spectra

In transition 3d metal compounds, cation L X-ray absorption spectra are dominated by intra-atomic and short-range effects. In view of this, metal L X-ray absorption spectra correspond to the metal 2p → metal valence band (3d) transitions and are determined by the valence state of metal atoms. Ti $L_{2,3}$ X-ray absorption spectra of anatase $Ti_{0.97}Co_{0.03}O_2$ nanopowders are shown in Fig. 3. Spectral features labeled A, B, C, D, and E are related to the Ti L_3 line. The Ti L_2 line consists of features F and G. The Ti L_3 and L_2 lines are split in the crystal field in t_{2g} (features A, B/C, and F) and e_g (features D and E).[32–34]

According calculations of de Groot et al.,[35,36] the distance between t_{2g} and e_g related

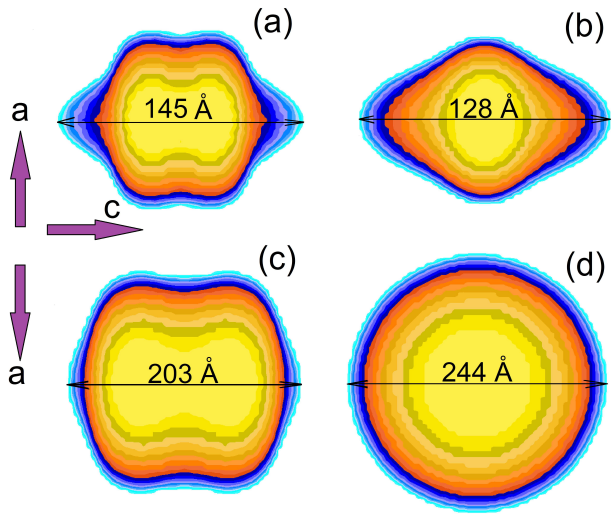

Figure 2: Visualization of the diffraction domain represented as a 2D projection on the ac crystallographic plane for (a) as-synthesized TiO_2 sample, (b) as-synthesized $Ti_{0.97}Co_{0.03}O_2$ sample, (c) $Ti_{0.97}Co_{0.03}O_2$ sample annealed in vacuum, (d) $Ti_{0.97}Co_{0.03}O_2$ sample annealed in hydrogen. Apparent domain size along c direction calculated from the integral breadth of the (004) Bragg peak is shown on the figures.

peaks in Ti $L_{2,3}$ XAS spectra does not equal exact to the crystal field splitting 10Dq since these spectra are strongly affected by correlation effects. The additional splitting of the higher-energy peaks for each line (peaks D and G) is due to distortion of the coordination environment.[32,37] The pre-edge features A and B are due to 2p–3d multiplet interactions.[37] Note that relative intensities of the peaks D and E are reversed for TiO_2 in rutile and anatase structures.[38,39] In Ti L_3 spectra of anatase TiO_2, the peak D is more intense than the peak E. Therefore, all the samples have the anatase structure. Small blurring of the spectral area between the D and E peaks for the as synthesized $Ti_{0.97}Co_{0.03}O_2$ sample is a characteristic of its partial amorphization. The spectra of the samples annealed in vacuum or hydrogen are characterized by more pronounced splitting of the e_g states. It means that the content of the amorphous phase decreases.

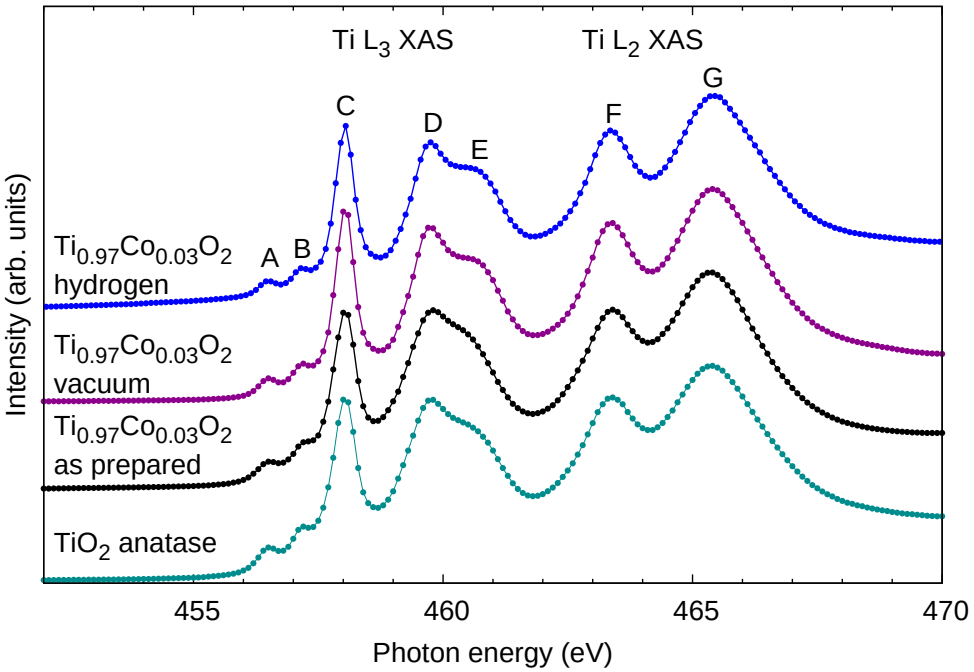

Figure 3: Ti $L_{2,3}$ X-ray absorption spectra of anatase TiO_2 and $Ti_{0.97}Co_{0.03}O_2$ nanopowders in the as-prepared state and after annealing in vacuum and hydrogen.

X-ray absorption Co $L_{2,3}$ spectra

The degree of oxidation of cobalt impurity ions in anatase TiO_2 can be estimated from Co $L_{2,3}$ absorption spectra shown in Fig. 4. In addition, here are present the spectra of single-crystal CoO and metallic cobalt. The results of crystal-field multiplet calculations of $L_{2,3}$ XAS spectra for Co ions in oxygen octahedral (O_h) and tetrahedral (T_d) environments are presented too. The crystal field parameters 10Dq were taken equal to 0.8 eV and -0.6 eV for the octahedral and tetrahedral environments, respectively.

The Co L spectra of titanium dioxide nanopowders do not correspond to either the spectra of CoO or metallic Co. The experimental Co $L_{2,3}$ spectra are well described by multiplets for Co^{2+} ions in tetrahedral oxygen environment (T_d, $10Dq = -0.6$ eV). Therefore, Co^{2+} ions are mainly in tetrahedra. Nevertheless, some cobalt ions are located in octahedra. This is indicated by the low-energy feature at about 777.5 eV which is reproduced in multiplet calculations for cobalt ions in octahedra. Annealing the sample in vacuum or hydrogen does

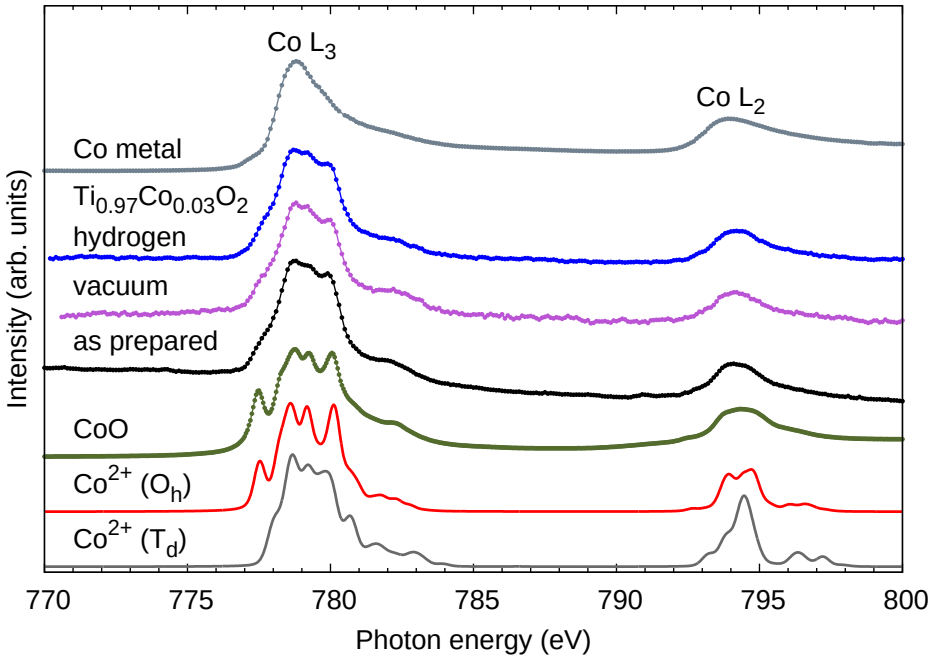

Figure 4: Co $L_{2,3}$ X-ray absorption spectra of single-crystal CoO, metallic Co and nanopowders $Ti_{0.97}Co_{0.03}O_2$ before and after annealing in vacuum and hydrogen. The spectra are normalized to the intensities of the Co L_3 maxima. For comparison, the spectra of CoO, metallic Co, and the results of calculations of the atomic multiple for Co^{2+} ions in the oxygen octahedral (O_h) and tetrahedral (T_d) environments are presented.

not change its spectra. No traces of metallic cobalt were found.

Co K X-ray absorption spectra

The Co K-edge X-ray absorption spectra of $Ti_{0.97}Co_{0.03}O_2$ nanopowders before and after annealing in vacuum and hydrogen are presented in Fig. 5. For comparison, Co K XAS spectra of metal cobalt and CoO are shown also.

The main peak B of the Co K edge X-ray absorption spectra of Co compounds should be interpreted as the electric dipole transition of core 1s electrons into the 4p empty states.[40] The small pre-edge structure at about 7711 eV (feature A) can be describe as the quadrupole electron transition Co 1s $\rightarrow$ Co 3d.[41] This transition occurs due to hybridization between the Co 3d and O 2p bands. Therefore, this pre-peak mainly reflects the density of empty Co 3d orbitals via hybridization with oxygen atoms. The first peak A′ in the spectrum of

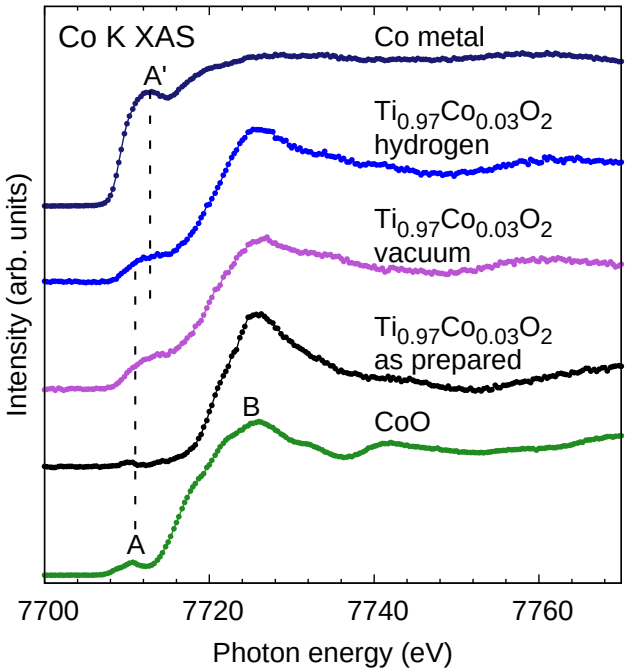

Figure 5: Co K X-ray absorption spectra in high-resolution fluorescence (HERFD) mode of $Ti_{0.97}Co_{0.03}O_2$ nanopowders before and after annealing in vacuum and hydrogen. For comparison, spectra of metallic Co and CoO are presented.

metallic Co is more intense and it is shifted toward the high-photon-energy region relative to the peak A of the spectrum of CoO. The feature A′ can be serve as a characteristic of the metallic state of cobalt.

The spectrum of the as-prepared $Ti_{0.97}Co_{0.03}O_2$ sample differs essentially from that of CoO and metallic Co. In contrast to Co $L_{2,3}$ spectra, Co K spectra of the $Ti_{0.97}Co_{0.03}O_2$ sample are changed after annealing the sample in vacuum or in hydrogen. The spectra of the annealed sample show features which are specific for the spectrum of metallic Co. For example, the pre-edge features is more intense and shifted toward the high-photon energies.

Annealing the sample in vacuum and hydrogen does completely restore the part of cobalt to the metallic state. This can be seen from the comparison of the Co K-spectrum of a sample annealed in vacuum and in hydrogen and the Co K spectrum of metallic cobalt. It should be noted that the presence of metallic cobalt in $Ti_{0.97}Co_{0.03}O_2$ nanopowders after annealing in vacuum and in hydrogen is also confirmed by X-ray diffraction data.

Resonant inelastic X-ray scattering spectra at the Co K edge

For visualization of Co K XAS data measured in HERFD mode, we have carried out measurements of resonant inelastic X-ray scattering (RIXS) data of the $Ti_{0.97}Co_{0.03}O_2$ samples near the Co K edge using Co K$\beta_{1,3}$ fluorescence. For Co oxides, Co 1s3p (Co K$\beta_{1,3}$) RIXS spectra were presented in works of Ding et al.[42] and Samarai et al.[43]

The RIXS data of CoO, Co-metal and $Ti_{0.97}Co_{0.03}O_2$ before and after annealing are depicted in Fig. 6 as a color plane of incident and transferred photon energies The vertical axis represents the energy difference between the incident and emitted energies. Variations of the color on the plot correspond to the different scattering intensities. High-intense spectral features are shown in red and low-intense areas are painted in blue. An enlarged pre-edge part of the RIXS spectra of CoO and as-prepared $Ti_{0.97}Co_{0.03}O_2$ sample are shown in Fig. 7. In order to make the pictures more pronounce, the color palette was changed. The RIXS data is in an excellent agreement with those published by Samarai et al.[43] The spectral features of CoO are shifted from the diagonal of the RIXS plane. Two energy-loss features A_1 and A_2 in the spectrum of CoO for the incident energy of 7710 eV (Fig. 7) should be related to the 3p–3d exchange splitting in the $3p^5 3d^7$ final state.[43] The same features are seen in the spectrum of the as-prepared $Ti_{0.97}Co_{0.03}O_2$ sample. All pre-edge features of the spectrum of Co metal lie on the diagonal of the RIXS plane. The complete understanding of the RIXS spectra requires an elaborate theoretical analysis, which is beyond the scope of the present paper.

The pre-peak features in the spectra of the annealed $Ti_{0.97}Co_{0.03}O_2$ samples are situated on the diagonal of the RIXS plane. It is closer to the Co-metal behavior than to that of CoO. The RIXS measurements confirm the conclusion made from the diffraction and Co K XAS experiments that the annealed samples of $Ti_{0.97}Co_{0.03}O_2$ content some amount of Co atoms in the metallic state.

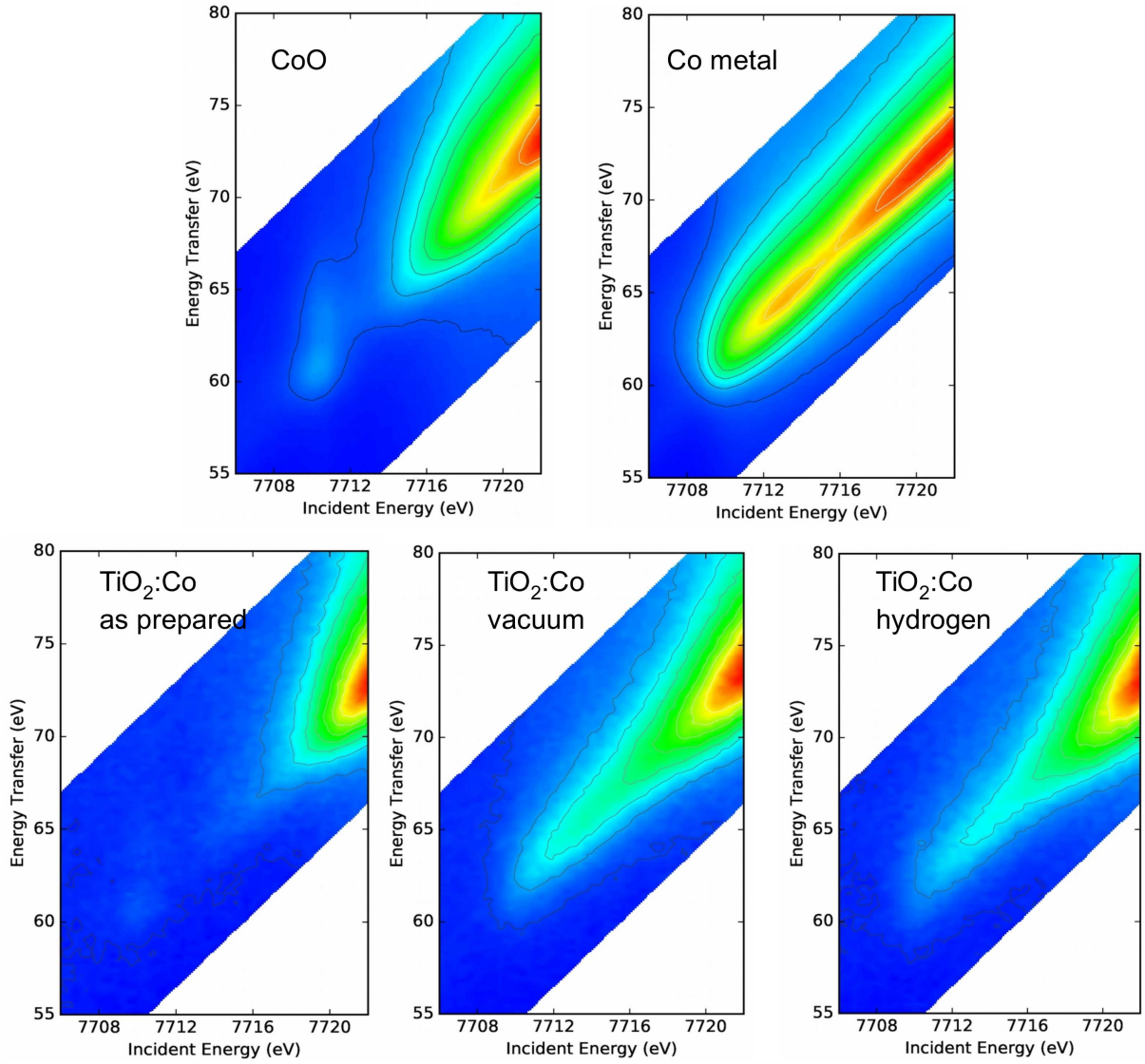

Figure 6: 1s3p ($K\beta_{1,3}$) RIXS plane at the Co K pre-edge of CoO, Co metal, and $Ti_{0.97}Co_{0.03}O_2$ (TiO_2:Co) nanopowders before and after annealing in vacuum and hydrogen.

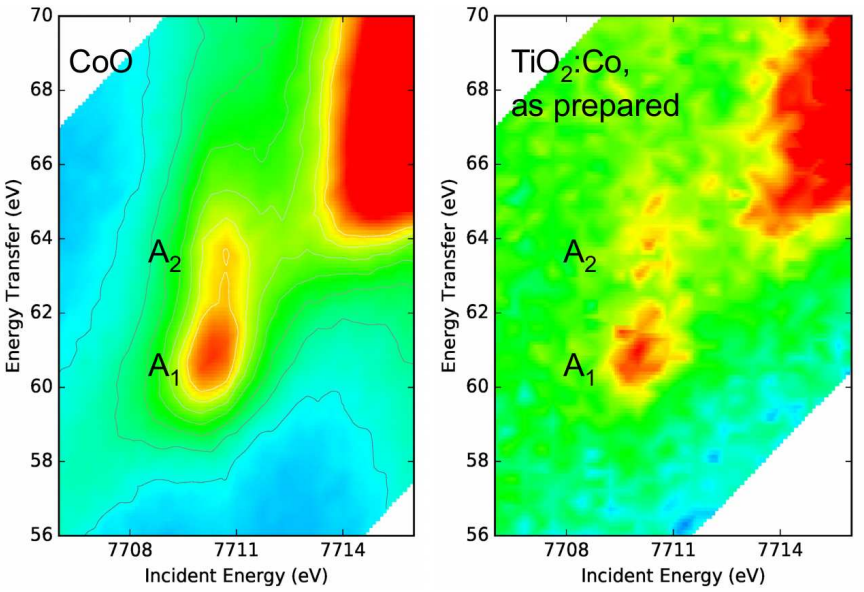

Figure 7: 1s3p RIXS ($K\beta_{1,3}$) plane at the Co K pre-edge of CoO and $Ti_{0.97}Co_{0.03}O_2$ nanopowders (as prepared).

Discussion

The analysis of the X-ray diffraction data for pure TiO_2 and as-prepared $Ti_{0.97}Co_{0.03}O_2$ nanopowder samples (see Table 1) revealed that doping of Co atoms in the anatase structure affects the unit cell parameters implying distortion of the crystal lattice. Moreover, it does not substantially affect the size of diffraction domains while microstrain effect was found to be twice higher for the Co-doped sample. As it has been reported by Rodríguez-Talavera et al.,[44] dopant atoms may be introduced in the TiO_2 anatase structure substitutionally or interstitially depending on the ionic radius. The substitution of Co^{2+} (high-spin state octahedral ionic radius = 0.885 Å) for Ti^{4+} (octahedral ionic radius = 0.745 Å) in the TiO_6 octahedra of the anatase structure produces vacancies over anion O^{2-} sublattice and may give rise to the lattice distortion as well as enhanced microstrain effect. As it has been shown by Li et al.,[45] tetrahedrally coordinated Ti^{4+} sites in pure nanocomposite TiO_2 with anatase structure emerge on the surface of nanoparticles as a precursor of anatase-to-rutie phase transformation. In that case Co^{2+} for Ti^{4+} substitution on the surface of nanoparticles would place cobalt ions in the thetrahedral environment. The X-ray absorption spectroscopy

data measured in total electron-yield mode, which revealed Co^{2+} ions in thetrahedral oxygen coordination, are in agreement with this scenario since it is surface sensitive method with an information depth of about 50–100 Å.

The second plausible scenario is that Co^{2+} ions partially occupy tetrahedrally coordinated interstices in the anatase structure forming Co–Ti^{3+}–V_O complexes. Here, V_O denotes a vacancy on an oxygen site. A possibility of localization of cobalt ions in interstices of anatase was discussed in the works by Roberts et al.[8] and Amadellu et al.[46] It was shown for rutile TiO_2:Co thin film on the base of measurements of Co K X-ray absorption spectra and first-principles calculations that the $Co_{Ti^{2+}}$–V_O complex was formed by the substitutional $Co_{Ti^{2+}}$ ions and O vacancy generated in the annealing process.[10]

The interatomic distances between the oxygen atoms in a tetrahedron on the surface of anatase nanoparticles are close to those reported for oxygen tetrahedra in Co_3O_4, where the cobalt ions are tetrahedrally coordinated.[47] An energy benefit of such arrangement of divalent cobalt ions is confirmed by calculations of density of states of cobalt doped TiO_2 anatase.[48] Therefore, one can conclude that Co^{2+} ions may be located in tetrahedral (T_d) oxygen environments, both replacing titanium ions and settling in interstitial sites of the anatase structure.

Annealing of the $Ti_{0.97}Co_{0.03}O_2$ nanopowder sample in vacuum or hydrogen atmosphere results in: (i) weakening of the microstrain effect and substantial increase of the size of diffraction domains; (ii) emergence of the Bragg lines of rutile TiO_2 and metallic Co phases on the X-ray diffraction patterns; (iii) evolution of the unit cell parameters towards the values reported for the bulk anatase structure $a(TiO_2) = 3.7848$ Å, $c(TiO_2) = 9.5124$ Å[27] (iv) change of the Ti $L_{2,3}$ X-ray absorption spectra which means that the content of the amorphous phase decreases; (v) appearance of signals from metallic Co in the Co K X-ray absorption and Co 1s3p RIXS spectra.

It is necessary to clarify the charge cobalt state in Co-doped anatase TiO_2 nanopowders subjected to annealing in vacuum or hydrogen. According to our X-ray spectroscopy

experiments, tetrahedrally coordinated cobalt ions are in the 2+ oxidation state in all the $Ti_{0.97}Co_{0.03}O_2$ samples, which is well agree with the recently reported results of X-ray absorption studies on $Ti_{0.98}Co_{0.02}O_2$.[49] On the other hand, X-ray diffraction data and results of the hard X-ray absorption spectroscopy measurements on the annealed samples indicate emergence of metallic cobalt. The controversy between these results can be resolved if we take into account information depth of our experiments.

Soft X-ray absorption spectra measured in total electron-yield mode are surface sensitive with an information depth of about 50–100 Å. This value is commensurable with the particle size. X-ray diffraction and hard X-ray spectroscopy are bulk information methods: they allow to explore micrometer ranges. We suggest that high temperature triggers diffusion of cobalt atoms from inside of the $Ti_{0.97}Co_{0.03}O_2$ nanoparticles to its surface, which affects the unit cell parameters and reduces microstrainn effect in the anatase phase. The diffusion of cobalt is followed by recrystallization processes and tendency of nanoparticles to form agglomerates. Such agglomerates formed by nanoparticles exist, for example, in nanostructured powders of manganites.[50–52] In this way, a soft X-ray spectroscopy to probe a surface part of the agglomerates which is rich of cobalt ions in the 2+ oxidation state. Contrary, hard X-ray spectroscopy is the in-depth probe for the nanoparticles agglomerates, which seems to incorporate metallic cobalt grains large enough to be observed by X-ray diffraction.

Conclusions

Cobalt-doped anatase $Ti_{0.97}Co_{0.03}O_2$ nanopowders (with a particle size of 10 nm) were produced by the hydrothermal synthesis method. Oxidation state of cobalt and titanium ions of the synthesized compounds were examined using hard and soft X-ray absorption spectra. Using surface sensitive soft X-ray absorption Co $L_{2,3}$ spectra in total electron yield mode it was found that cobalt ions in nanoparticles located on the surface of agglomerates are in the oxidation state 2+ with tetrahedral oxygen coordination, with titanium ions having

a tetravalent state of Ti^{4+}. Using bulk-sensitive Co Kβ resonant inelastic X-ray scattering (RIXS) spectra it was found that annealing in vacuum and hydrogen leads to clustering metal cobalt at the particles from the volume of agglomerates. According to the Ti L2, 3 and O K X-ray absorption spectra, all the samples before the thermal treatment contain an amorphous phase of titanium dioxide on the surface. After annealing in vacuum or hydrogen anatase structure of $Ti_{0.97}Co_{0.03}O_2$ remains and the amorphous phase disappears.

Acknowledgment

This work was supported by the Russian Scientific Foundation (grant No. 16-12-10004). VRG acknowledges financial supports of the Russian Foundation for Basic Research (Grant No. 16-02-00577) and FASO of Russia (theme "Electron" No 01201463326). The soft X-ray absorption measurements were carried out according to the bilateral Program "Russian-German Laboratory at BESSY", Berlin, Germany (Project 16103257-ST). The hard X-ray absorption and RIXS experiments were performed on beamline BM20 at the European Synchrotron Radiation Facility (ESRF), Grenoble, France (Project HC-2890). X-ray diffraction studies were performed using facilities of the shared access center "Composition of compounds" IHTE, UB RAS.

References

(1) Ohno, H. Making Nonmagnetic Semiconductors Ferromagnetic. *Science* **1998**, *281*, 951–956.

(2) Dietl, T.; Ohno, H.; Matsukura, F.; Cibert, J.; Ferrand, D. Zener Model Description of Ferromagnetism in Zinc-Blende Magnetic Semiconductors. *Science* **2000**, *287*, 1019–1022.

(3) Matsumoto, Y.; Murakami, M.; Shono, T.; Hasegawa, T.; Fukumura, T.; Kawasaki, M.;

Ahmet, P.; Chikyow, T.; Koshihara, S.-y.; Koinuma, H. Room-Temperature Ferromagnetism in Transparent Transition Metal-Doped Titanium Dioxide. *Science* **2001**, *291*, 854–856.

(4) Kim, D. H. et al. Formation of Co Nanoclusters in Epitaxial $Ti_{0.96}Co_{0.04}O_2$ Thin Films and Their Ferromagnetism. *Appl. Phys. Lett.* **2002**, *81*, 2421–2423.

(5) Coey, J. M. D.; Venkatesan, M.; Fitzgerald, C. B. Donor Impurity Band Exchange in Dilute Ferromagnetic Oxides. *Nat. Mater.* **2005**, *4*, 173–179.

(6) Rubensson, J. E. RIXS Dynamics for Beginners. *J. Electr. Spectr. Rel. Phen.* **2000**, *110–111*, 135–151.

(7) de Groot, F. M. F. High-Resolution X-ray Emission and X-ray Absorption Spectroscopy. *Chem. Rev.* **2001**, *101*, 1779–1808.

(8) Griffin Roberts, K.; Varela, M.; Rashkeev, S.; Pantelides, S. T.; Pennycook, S. J.; Krishnan, K. M. Defect-Mediated Ferromagnetism in Insulating Co-Doped Anatase TiO_2 Thin Films. *Phys. Rev. B* **2008**, *78*, 014409.

(9) Yildirim, O.; Cornelius, S.; Smekhova, A.; Zykov, G.; Gan'shina, E. A.; Granovsky, A. B.; Hubner, R.; Bahtz, C.; Potzger, The Local Environment of Cobalt in Amorphous, Polycrystalline and Epitaxial Anatase TiO_2:Co Films Produced by Cobalt Ion Implantation. *J. Appl. Phys.* **2015**, *117*, 183901.

(10) Yan, W. et al. Oxygen Vacancy Effect on Room-Temperature Ferromagnetism of Rutile Co:TiO_2 Thin Films. *Appl. Phys. Lett.* **2009**, *94*, 042508.

(11) de Souza, T. E.; Mesquita, A.; de Zevallos, A. O.; Beron, F.; Pirota, K. R.; Neves, P. P.; Doriguetto, A. C.; de Carvalho, H. B. Structural and Magnetic Properties of Dilute Magnetic Oxide Based on Nanostructured Co-Doped Anatase TiO_2 ($Ti_{1-x}Co_xO_{2-\delta}$). *J. Phys. Chem. C* **2013**, *117*, 13252–13260.

(12) Jeong, B.-S.; Heo, Y. W.; Nortona, D. P.; Hebard, A. F.; Budai, J. D.; Park, Y. D. Properties of Anatase $Co_xTi_{1-x}O_2$ Thin Films Epitaxially Grown by Reactive Sputtering. *Thin Solid Films* **2005**, *488*, 194–199.

(13) Kim, J.-Y. et al. Ferromagnetism Induced by Clustered Co in Co-Doped Anatase TiO_2 Thin Films. *Phys. Rev. Lett.* **2003**, *90*, 017401.

(14) Leedahl, B. et al. Study of the Structural Characteristics of 3d Metals Cr, Mn, Fe, Co, Ni, and Cu Implanted in ZnO and TiO_2 — Experiment and Theory. *J. Phys. Chem. C* **2014**, *118*, 28143–28151.

(15) Liu, L. F.; Kang, J. F.; Wang, Y.; Tang, H.; Kong, L. G.; Sun, L.; Zhang, X.; Han, R. The Influence of Hydrogen Annealing on Magnetism of Co-Doped TiO_2 Films Prepared by Sol-Gel Method. *J. Magn. Magn. Mater.* **2007**, *308*, 85–89.

(16) Mamiya, K.; Koide, T.; Fujimori, A.; Tokano, H.; Manaka, H.; Tanaka, A.; Toyosaki, H.; Fukumura, T.; Kawasaki, M. Indication of Intrinsic Room-Temperature Ferromagnetism in $Ti_{1-x}Co_xO_{2-\delta}$ Thin Film: An X-Ray Magnetic Circular Dichroism Study. *Appl. Phys. Lett.* **2006**, *89*, 062506.

(17) Pärna, R.; Joost, U.; Nũmmiste, E.; Käämbre, T.; Kikas, A.; Kuusik, I.; Hirsimäki, M.; Kink, I.; Kisand, V. Effect of Cobalt Doping and Annealing on Properties of Titania Thin Films Prepared by Sol-Gel Process. *Appl. Surf. Sci.* **2011**, *257*, 6897–6907.

(18) Thompson, P.; Cox, D. E.; Hastings, J. B. Rietveld Refinement of Debye-Scherrer Synchrotron X-ray Data from Al_2O_3. *J. Appl.Crystallogr.* **1987**, *20*, 79–83.

(19) Rodríguez-Carvajal, J. Recent Advances in Magnetic Structure Determination by Neutron Powder Diffraction. *Physica B* **1993**, *192*, 55–69.

(20) Caglioti, G.; Paoletti, A.; Ricci, F. P. Choice of Collimators for a Crystal Spectrometer for Neutron Diffraction. *Nuclear Instruments* **1958**, *3*, 223–228.

(21) González-Platas, J.; Rodríguez-Carvajal, J.; Fourier, G. A Windows/Linux Program to Calculate and Display Fourier Maps. http://www.ill.eu/sites/fullprof/index.html, 2000–2004.

(22) Bauer, M. HERFD-XAS and Valence-to-Core-XES: New Tools to Push the Limits in Research with Hard X-Rays? *Phys. Chem. Chem. Phys.* **2014**, *16*, 13827–13837.

(23) Stavitski, E.; de Groot, F. CTM4XAS 3.1 — Charge Transfer Multiplet Calculations for X-Ray Absorption Spectroscopy: Simulations of XAS, XPS and XES, Spectra of Transition Metal Systems. Utrecht University, 2010.

(24) Stavitski, E.; de Groot, F. M. The CTM4XAS Program for EELS and XAS Spectral Shape Analysis of Transition Metal L Edges. *Micron* **2010**, *41*, 687–694.

(25) Okada, K.; Kotani, A. Complementary Roles of Co 2p X-Ray Absorption and Photoemission Spectra in CoO. *J. Phys. Soc. Jpn.* **1992**, *61*, 449–453.

(26) de Groot, F. M. F.; Abbate, M.; van Elp, J.; Sawatzky, G. A.; Ma, Y. J.; Chen, C. T.; Sette., F. Oxygen 1s and Cobalt 2p X-Ray Absorption of Cobalt Oxides. *J. Phys.: Condens. Matter.* **1993**, *5*, 2277–2288.

(27) Burdett, J. K.; Hughbanks, T.; Miller, G. J.; Richardson, J. W.; Smith, J. V. Structural-Electronic Relationships in Inorganic Solids: Powder Neutron Diffraction Studies of the Rutile and Anatase Polymorphs of Titanium Dioxide at 15 and 295 K. *Journal of the American Chemical Society* **1987**, *109*, 3639–3646.

(28) Rodríguez-Carvajal, J. Recent Developments of the Program FULLPROF. *Commission on powder diffraction (IUCr). Newsletter* **2001**, *26*, 12–19.

(29) Rodríquez-Carvajal, J.; Roisnel, T. Line Broadening Analysis Using FullProf*: Determination of Microstructural Properties. European Powder Diffraction EPDIC 8. 2004; pp 123–126.

(30) Stokes, A. R.; Wilson, A. J. C. The Diffraction of X Rays by Distorted Crystal Aggregates - I. *Proceedings of the Physical Society* **1944**, *56*, 174.

(31) Järvinen, M. Application of Symmetrized Harmonics Expansion to Correction of the Preferred Orientation Effect. *Journal of Applied Crystallography* **1993**, *26*, 525–531.

(32) de Groot, F. M. F.; Figueiredo, M. O.; Basto, M. J.; Abbate, M.; Petersen, H.; Fuggle, J. C. 2*p* X-Ray Absorption of Titanium in Minerals. *Phys. Chem. Minerals* **1992**, *19*, 140–147.

(33) Stoyanov, E.; Langenhorst, F.; Steinle-Neumann, G. The Effect of Valence State and Site Geometry on Ti $L_{3,2}$ and O K Electron Energy-Loss Spectra of Ti_xO_y Phases. *Amer. Mineralogist* **2007**, *92*, 577–586.

(34) Krüger, P. Multichannel Multiple Scattering Calculation of $L_{2,3}$-Edge Spectra of TiO_2 and $SrTiO_3$: Importance of Multiplet Coupling and Band Structure. *Phys. Rev. B* **2010**, *81*, 1251.

(35) de Groot, F. M. F.; Fuggle, J. C.; Thole, B. T.; Sawatzky, G. A. $L_{2,3}$ X-Ray-Absorption Edges of d^0 Compounds: K^+, Ca^{2+}, Sc^+, and Ti^+ in O_h (Octahedral) Symmetry. *Phys. Rev. B* **1990**, *41*, 928–937.

(36) de Groot, F. M. F.; Faber, J.; Michiels, J. J. M.; Czyżyk, M. T.; Abbate, M.; Fuggle, J. C. Oxygen 1*s* X-Ray Absorption of Tetravalent Titanium Oxides: A Comparison with Single-Particle Calculations. *Phys. Rev. B* **1993**, *48*, 2074–2080.

(37) Crocombette, J. P.; Jollet, F. Ti 2p X-Ray Absorption in Titanium Dioxides (TiO_2): the Influence of the Cation Site Environment. *J. Physics: Cond. Matter* **1994**, *6*, 10811–10821.

(38) Henderson, G. S.; Liu, X.; Fleet, M. E. A Ti L-Edge X-Ray Absorption Study of Ti-Silicate Glasses. *Physics and Chemistry of Minerals* **2002**, *29*, 32–42.

(39) Kucheyev, S. O.; van Buuren, T.; Baumann, T. F.; Satcher, J. H.; Willey, T. M.; Meulenberg, R. W.; Felter, T. E.; Poco, J. F.; Gammon, S. A.; Terminello, L. J. Electronic Structure of Titania Aerogels from Soft X-Ray Absorption Spectroscopy. *Phys. Rev. B* **2004**, *69*, 245102.

(40) Pandey, S. K.; Kumar, A.; Khalid, S.; Pimpale, A. V. Electronic States of $LaCoO_3$: Co K-Edge and La L-Edge X-Ray Absorption Studies. *Journal of Physics: Condensed Matter* **2006**, *18*, 7103–7114.

(41) Medarde, M.; Dallera, C.; Grioni, M.; Voigt, J.; Podlesnyak, A.; Pomjakushina, E.; Conder, K.; Neisius, T.; Tjernberg, O.; Barilo, S. N. Low-Temperature Spin-State Transition in $LaCoO_3$ Investigated Using Resonant X-Ray Absorption at the Co K Edge. *Phys. Rev. B* **2006**, *73*, 054424.

(42) Ding, Y.; Fernandez-Rodríguez, J.; Kim, J.; Li, F.; Casa, D.; Upton, M.; Gog, T.; Mao, H.-k.; van Veenendaal, M. Spin-Ordering Mediated Orbital Hybridization in CoO at High Pressures. *Phys. Rev. B* **2012**, *86*, 094107.

(43) Samarai, M. A.; Delgado-Jaime, M. U.; Ishii, H.; Hiraoka, N.; Tsuei, K.-D.; Rueff, J.-P.; Lassale-Kaiser, B.; Weckhuysen, B. M.; de Groot, F. M. $1s3p$ Resonant Inelastic X-Ray Scattering of Cobalt Oxides and Sulfides. *J. Phys. Chem. C* **2016**, *120*, 24063–24069.

(44) Rodríguez-Talavera, R.; Vargas, S.; Arroyo-Murillo, R.; Montiel-Campos, R.; Haro-Poniatowski, E. Modification of the Phase Transition Temperatures in Titania Doped with Various Cations. *Journal of Materials Research* **1997**, *12*, 439–443.

(45) Li, G.; Dimitrijevic, N. M.; Chen, L.; Nichols, J. M.; Rajh, T.; Gray, K. A. The Important Role of Tetrahedral Ti^{4+} Sites in the Phase Transformation and Photocatalytic Activity of TiO_2 Nanocomposites. *Journal of the American Chemical Society* **2008**, *130*, 5402–5403.

(46) Amadelli, R.; Samiolo, L.; Maldotti, A.; Molinari, A.; Valigi, M.; Gazzoli, D. Preparation, Characterisation, and Photocatalytic Behaviour of Co-TiO_2 with Visible Light Response. *Intern. J. Photoenergy* **2008**, 853753.

(47) Müller, S. Synchrotron Radiation Spectroscopy Studies of the Initial Interaction of Chromium and Cobalt with the Surface of Titanium Dioxide. Ph.D. thesis, 2010.

(48) Geng, W. T.; Kim, K. S. Interplay of Local Structure and Magnetism in Co-Doped TiO_2 Anatase. *Solid State Commun.* **2004**, *129*, 741–746.

(49) Mesilov, V. V.; Galakhov, V. R.; Udintseva, M. S.; Yermakov, A. Y.; Uimin, M. A.; Smirnov, D. A.; Gubkin, A. F.; Sherstobitova, E. A. Soft X-Ray Absorption Spectroscopy of Titanium Dioxide with Cobalt Impurities. *J. Experim. Theoret. Physics* **2017**, *151*, 1066–1072.

(50) Mostovshchikova, E. V.; Loshkareva, N. N.; Telegin, A. V.; Naumov, S. V.; Gizhevskii, B. A.; Naumova, L. I. Large Infrared Magnetotransmission Effect in Composite and Nano-Composite Based on $Nd_{0.5}Sr_{0.5}MnO_3$. *J. Appl. Phys.* **2013**, *113*, 043503.

(51) Galakhov, V. R.; Mesilov, V. V.; Shamin, S. N.; Gizhevskii, B. A.; Skorikov, N. A.; Naumov, S. V.; Vilkov, O. Y. X-Ray Spectra and Valence States of Cations in Nanostructured Half-Doped $La_{0.5}Ca_{0.5}MnO_3$ Manganite. *Appl. Phys. A* **2015**, *118*, 649–654.

(52) Fabre, A.; Salameh, S.; Ciacchi, L. C.; Kreutzer, M. T.; van Ommen, J. R. Contact Mechanics of Highly Porous Oxide Nanoparticle Agglomerates. *J. Nanopart. Res.* **2016**, *18*, 200.